

Antitumor Effects of Apatinib on Tongue Cancer in Patient-Derived Xenograft Models

Yiping Sun^{1,2,3}, MD; Yuqi Xin⁴, PhD; Yuanqiao He⁵, PhD; Junyao Liu^{1,2,3}, MSc; Xiaoping Hu^{1,2,3}, PhD¹

¹The Affiliated Stomatological Hospital, Jiangxi Medical College, Nanchang University, Nanchang, Jiangxi, China;

²Jiangxi Province Key Laboratory of Oral Biomedicine, Nanchang, Jiangxi, China;

³Jiangxi Province Clinical Research Center for Oral Diseases, Nanchang, Jiangxi, China;

⁴Department of Stomatology, The First Affiliated Hospital, Jiangxi Medical College, Nanchang University, Nanchang, Jiangxi, China;

⁵Center of Laboratory Animal Science, Nanchang University, Nanchang, Jiangxi, China

Correspondence:

Xiaoping Hu, PhD;
The Affiliated Stomatological Hospital, Jiangxi Medical College, Nanchang University, Nanchang, Postal code: 330006, Jiangxi, China

Tel: +86 79186360817

Email: 563960724@qq.com

Received: 29 March 2025

Revised: 24 June 2025

Accepted: 08 August 2025

Abstract

Background: Tongue cancer is the most common malignant tumor in the oral and maxillofacial region. Novel effective therapies are urgently needed. Apatinib, a small-molecule antiangiogenic tyrosine kinase inhibitor, has demonstrated efficacy in gastric cancer, but its role in tongue cancer remains unclear. This study evaluated the antitumor effects and mechanisms of apatinib using patient-derived xenograft (PDX) models of tongue cancer.

Methods: Fresh tumor tissues from two tongue cancer patients (Affiliated Stomatological Hospital of Nanchang University, 2019-2021) were subcutaneously inoculated into immunodeficient mice to establish PDX models, validated by histology and human-specific gene identification. Eighteen P4-generation PDX mice were randomized into three groups (*n*=6/group): Control: 100 μ L/day saline (oral gavage), Cisplatin: 5 mg/Kg/week (intraperitoneal injection), Apatinib: 100 mg/Kg/day (oral gavage). After 21 days of treatment, tumor volume/weight was measured. Immunohistochemistry (IHC) assessed microvessel density (MVD, via CD31) and cell proliferation (Ki-67). Data were analyzed by one-way ANOVA with Tukey's *post hoc* test.

Results: Apatinib significantly inhibited tumor growth, reducing tumor weight (0.21 ± 0.07 g vs. Control 0.93 ± 0.30 g, $P=0.036$) and volume (211.32 ± 166.38 mm^3 vs. Control 800.98 ± 581.05 mm^3 , $P=0.0002$). IHC revealed decreased MVD (0.88 ± 0.07 vs. Control 4.30 ± 0.34 , $P=0.0192$) and Ki-67-positive cells ($2.75\%\pm0.28\%$ vs. Control $32.05\%\pm4.34\%$, $P=0.047$), indicating suppressed angiogenesis and proliferation. Mouse body weight remained stable, suggesting minimal toxicity.

Conclusion: Our findings revealed that apatinib significantly suppressed tumor growth in these models, accompanied by a reduction in tumor microvascular density and Ki-67 expression, indicating its potential mechanism of action through inhibiting angiogenesis and tumor cell proliferation. These findings support its potential as a targeted therapy for tongue cancer and highlight the utility of PDX models for preclinical drug evaluation. Further studies with larger cohorts are warranted to validate these results.

Please cite this article as: Sun Y, Xin Y, He Y, Liu J, Hu X. Antitumor Effects of Apatinib on Tongue Cancer in Patient-Derived Xenograft Models. Iran J Med Sci. 2026;51(2):145-153. doi: 10.30476/ijms.2025.106422.4059.

Keywords • Apatinib • Xenograft model antitumor assay • Tongue neoplasms • Platelet endothelial cell adhesion molecule-1 • Ki-67 antigen

Introduction

Tongue cancer is the most common malignant tumor in the oral and maxillofacial region.¹ It has a high incidence, poor clinical treatment efficacy, and a low patient survival rate.² Given the lack of robust

What's Known

- Patient-derived xenograft can reproduce the histological characteristics, tumor specificity, and tumor growth microenvironment of the primary tumor.
- Apatinib is a VEGFR-2 inhibitor that exhibits antitumor efficacy in advanced gastric cancer by suppressing angiogenesis.

What's New

- A critical component of our study involved the establishment of parallel patient-derived xenograft (PDX) models for non-keratinizing and keratinizing tongue squamous cell carcinomas. We assessed the efficacy of apatinib in these two distinct histological subtypes.

pre-clinical research models, investigations into the pathogenesis and therapeutic methods of tongue cancer are progressing slowly. New and effective treatment methods for use in clinical settings are urgently needed.

Patient-derived xenograft (PDX) models are animal models where the fresh tumor cells or tissues of patients are directly transplanted into immunodeficient mice orthotopically or ectopically; they rely on the mice to provide the environment for growth.^{3, 4} These models retain the microenvironment and histopathological and genetic characteristics of primary tumors, and they can be used to screen anticancer drugs and predict clinical efficacy.⁵

Apatinib is a small-molecule antiangiogenic targeted drug developed independently in China.⁶ It is the first drug that has been proven to be safe and effective in patients with advanced gastric cancer worldwide.⁷⁻⁹ Beyond gastric cancer, emerging evidence suggests that apatinib may hold therapeutic potential in other head and neck malignancies.¹⁰ While there have been initial investigations into the use of apatinib in the broader context of oral squamous cell carcinoma, such as a pilot study exploring the neoadjuvant combination of anti-PD-1 camrelizumab and the VEGFR2 inhibitor apatinib for locally advanced resectable oral squamous cell carcinoma.¹¹ However, studies specifically focusing on the treatment of tongue cancer are still limited, particularly regarding its efficacy in different histological subtypes of tongue squamous cell carcinoma.

This study aims to investigate the antitumor efficacy of apatinib in tongue cancer and uncover its underlying mechanisms through newly established patient-derived xenograft (PDX) models.

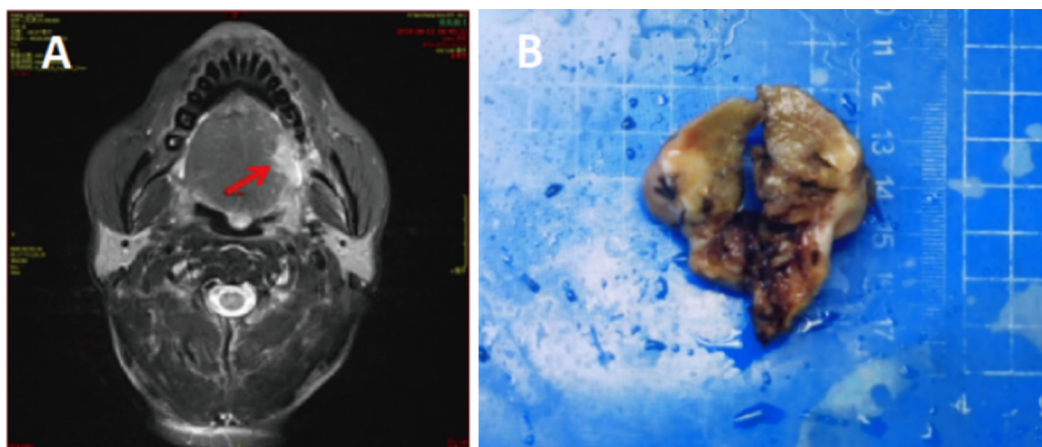


Figure 1: (A) Axial contrast-enhanced computed tomography (CT) image of Patient No. 1 (74-year-old male) demonstrates a solid, ill-defined mass (arrow) located at the left margin of the tongue. The lesion has invaded and destroyed the adjacent left alveolar bone. (B) Macroscopic photograph of the surgically resected tongue cancer specimen from Patient No. 1 (74-year-old male). The specimen shows the gross morphology of the primary tumor tissue used for establishing the patient-derived xenograft (PDX) models.

Materials and Methods

Tumor Samples

The fresh tumor samples were surgically removed from patients with tongue cancer at the Affiliated Stomatological Hospital of Nanchang University in 2019-2021 (figure 1). The first patient (No. 1) was a 74-year-old male with a pathologist's diagnosis of non-keratinizing squamous cell carcinoma of the tongue. The second patient (No. 2) was a 55-year-old male with a diagnosis of squamous carcinoma of the tongue. The patients signed informed consent, and the study was approved by the Ethics Committee of the Affiliated Stomatological Hospital of Nanchang University (Permit No. 2021068). Samples were quickly put into DMEM High Glucose Medium (Beyotime Biotechnology, Shanghai, China), and sent to the laboratory within 4 h at low temperature (2-8 °C).

Laboratory Animals

Female Balb/c nude mice (GemPharmatech Co., Ltd., Nanjing, Jiangsu, China) aged 6-8 weeks were selected. The mice were cared for according to the institutional guidelines for animal care. Mice were fed commercial mouse diet food with a 12-hour light-dark cycle under specific pathogen-free (SPF) conditions. Animal studies were approved by the Institutional Animal Care and Use Committee of Nanchang Royo Biotech Co., Ltd (Permit No. RYE2021020501). Standard animal care and laboratory guidelines are based on "Guidelines for the Care and Use of Laboratory Animals" (National Research Council, 8th edition, 2011).

Construction of PDX Models of Tongue Cancer

The fresh tumor tissue of tongue cancer was divided into 2×2×2 mm micro tissue blocks, then they were inoculated subcutaneously on the

mouse scapula with a trocar after administration of local anesthesia aseptically within <24 h. This sample was recorded as generation P0. When the tumor tissue had grown to 1000–1500 mm³, it was removed and passaged to P1–P4 using the same method. Eighteen P4 generation of PDX mice were used for subsequent experiments.

Hematoxylin–eosin (H&E) Staining

The tumor tissues of patients and PDX models were fixed in formalin, embedded in paraffin, cut into 4 µm paraffin sections, and stained with H&E by using an automatic slide stainer Dp360 (Dakewe, Dp360, Guangdong, China).

Polymerase Chain Reaction (PCR)

DNA from PDX model tissues and patients was extracted using DNeasy Blood & Tissue Kit (Qiagen #69504, Germany). Two pairs of human and mouse gene-specific primers were designed according to the housekeeping genes of humans and mice.¹² The extracted sample was amplified by PCR.

Drug Sensitivity of PDX Models

Eighteen P4 generation mice were randomly divided into three groups (n=6): 1) Control group: 100 µL/day normal saline, once a day, orally; 2) Cisplatin (Haosen, Jiangsu, China) group: 5 mg/Kg, once a week, intraperitoneal injection; and 3) Apatinib (Hengrui, Jiangsu, China) group: 100 mg/Kg,¹³ once a day, orally. The tumor volume and weight of mice were observed every 3 days. After 21 days of drug intervention, the mice were sacrificed, and the tumor tissues were stripped and weighed.

Immunohistochemical (IHC) Staining

Tissue samples of the PDX model were stained with anti-CD31 antibodies (MXB Biotechnologies, Fuzhou, China) to evaluate microvascular density (MVD) in the tumor and with anti-Ki67 antibodies (MXB Biotechnologies, Fuzhou, China) to calculate the tumor proliferation index. Single endothelial cells or a cluster of cells positive for CD31 were considered a vessel. For each specimen, the area with the largest number of microvessels was selected. The MVD was determined as follows:

$$\frac{\text{number of vessels}}{\text{analyzed tumor area}(\text{mm}^2)} \times 10^{-4}$$

For Ki-67 analysis, the positive cell rate was calculated as the ratio of the number of positive cells to the number of total cells.¹⁴

Statistical Analysis

The Statistical Package for the Social Sciences (SPSS) (version 22.0, IBM, Armonk,

New York, USA) and GraphPad Prism software (version 9.0, GraphPad Software, Inc., San Diego, California, USA) were used for data analysis. The results were expressed as mean±SD. Multi-group comparison was performed using one-way analysis of variance (ANOVA) and Tukey's *post hoc* test. The threshold of statistical significance was set at P<0.05.

Ethical Consideration

The study was conducted in accordance with the Declaration of Helsinki (as revised in 2013). The approval for this research was granted by the Ethics Committee of the Affiliated Stomatological Hospital of Nanchang University (Permit No. 2021068), and written informed consent was obtained from both participants. Animal studies were approved by the Institutional Animal Care and Use Committee of Nanchang Royo Biotech Co., Ltd (Permit No. RYE2021020501). Standard animal care and laboratory guidelines are based on "Guidelines for the Care and Use of Laboratory Animals" (National Research Council, 8th edition, 2011)

Results

Establishment and Identification of the PDX Tongue Cancer Model

Two PDX models of tongue cancer were successfully constructed. H&E staining showed that the PDX models were histologically consistent with the corresponding patients. They retained the characteristics of differentiation, keratosis, and nuclear atypia (figure 2).

After the PCR experiment, the results showed that the DNA of the PDX model tumor tissues contained both mouse and human target genes (figure 3). Thus, the transplanted tumor tissue was of human origin.

Apatinib Inhibits Tumor Growth

According to the tumor growth curve of each drug group, tumor growth was inhibited in all treatment groups. The tumor weight in the apatinib group (0.21±0.07 g) was significantly lighter than that in the control group (0.93±0.30 g) (P=0.036) and the cisplatin group (0.62±0.20 g) (P=0.0084) (figures 4 A and B). The tumor volume increment in the apatinib group (211.32±166.38 mm³) was significantly smaller than that in the control group (800.98±581.05 mm³) (P=0.0002) and the cisplatin group (582.15±442.17 mm³) (P=0.0028) (figure 4C). The body weight of the mouse was 2.58±0.87 g in the apatinib group, 3.70±1.17 g in the control group, and 2.20±1.04 g in the cisplatin group. However, the increment has no significant difference among the groups (figure 4D) (P=0.078).

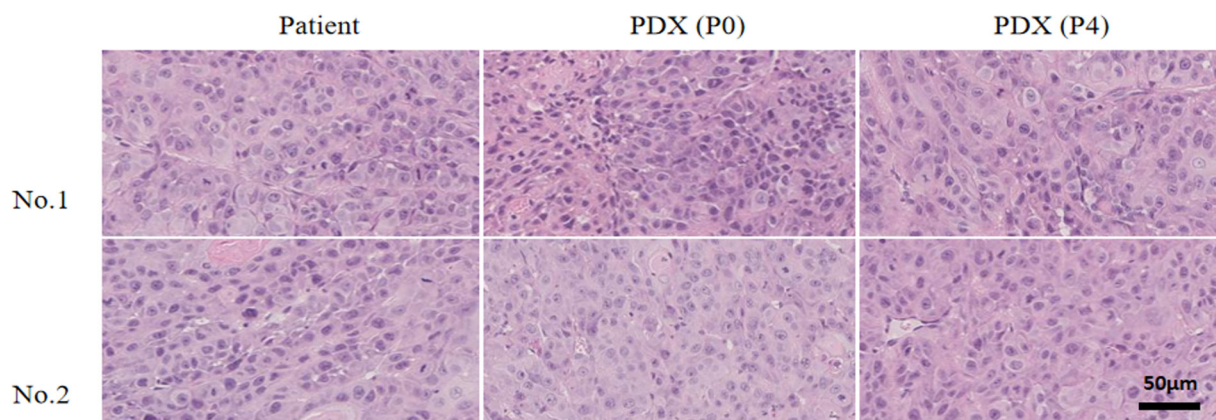


Figure 2: Photomicrographs of hematoxylin-eosin-stained tumor sections show that the pathological phenotypes of tumor tissues in patients and PDX models showed similar growth pattern and morphology to the original tumor ($\times 400$).

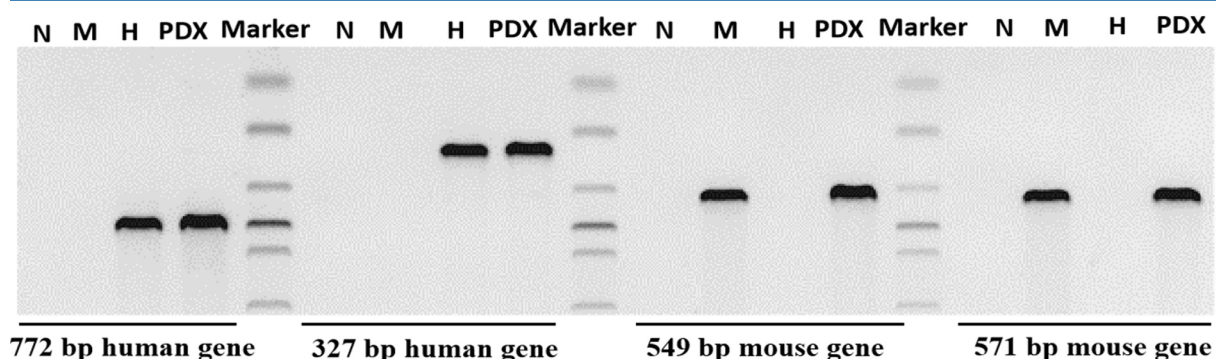


Figure 3: The picture depicts the results of a PCR analysis aimed at identifying human-derived genes in PDX model tissues. The gel electrophoresis image clearly shows bands corresponding to both human and mouse genes. Two distinct human gene bands are observed at approximately 772 base pairs (bp) and 327 bp, which are present in both the patient tissue (H) and the PDX samples, indicating the successful amplification of human DNA. Conversely, two mouse gene bands are visible at approximately 549 bp and 571 bp, which are present in the mouse positive control (M) but absent in the patient tissue. The negative control (N) lacks any bands, confirming the specificity of the PCR reaction.

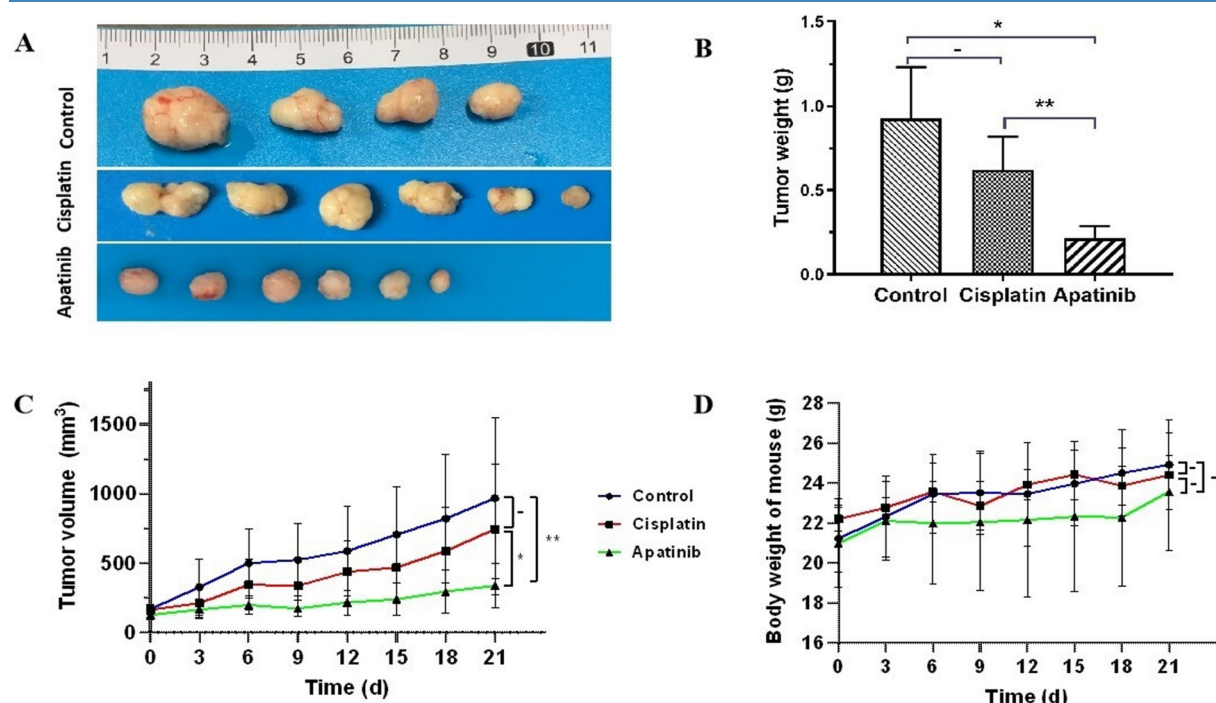


Figure 4: Antitumor Effects of Apatinib in Tongue Cancer PDX Models. (A) Photographs show the tumor volume of mice in all groups (Control, Cisplatin, Apatinib; $n = 6$ per group) after 21 days (B) Bar graph illustrates the tumor weight of mice in all groups, with significant differences observed between the apatinib group and both the control and cisplatin groups ($^*P=0.036$; $^{**}P=0.0084$). (C) The line graph depicts the tumor growth curve of mice. (D) The line graph shows the body weight of mice over time, with no significant difference in weight increment among the groups.

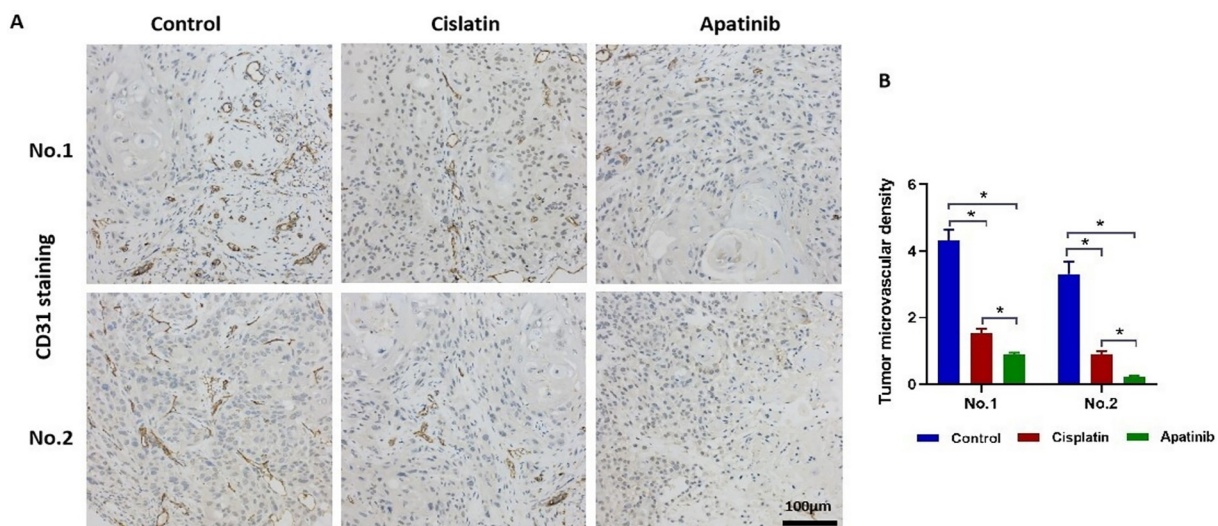


Figure 5: Apatinib Inhibits Angiogenesis in Tongue Cancer PDX Models (Assessed by Microvascular Density via CD31 Immunohistochemistry). (A) Representative images of immunohistochemical (IHC) staining for CD31-positive blood vessels in PDX model tumor tissues. The images show varying degrees of CD31 staining across the control, cisplatin, and apatinib treatment groups for two different patient samples (No. 1 and No. 2). The cytoplasm of vascular endothelial cells-stained pale brown or brown, can be considered a countable vessel ($\times 200$). (B) The bar graph illustrates the tumor microvascular density (MVD) in the various groups for both patient samples. The MVD values are significantly lower in the apatinib group compared to the control and cisplatin groups for both samples ($*P<0.05$).

Apatinib Inhibits Angiogenesis

inhibiting angiogenesis ($P=0.0192$) (figure 5).

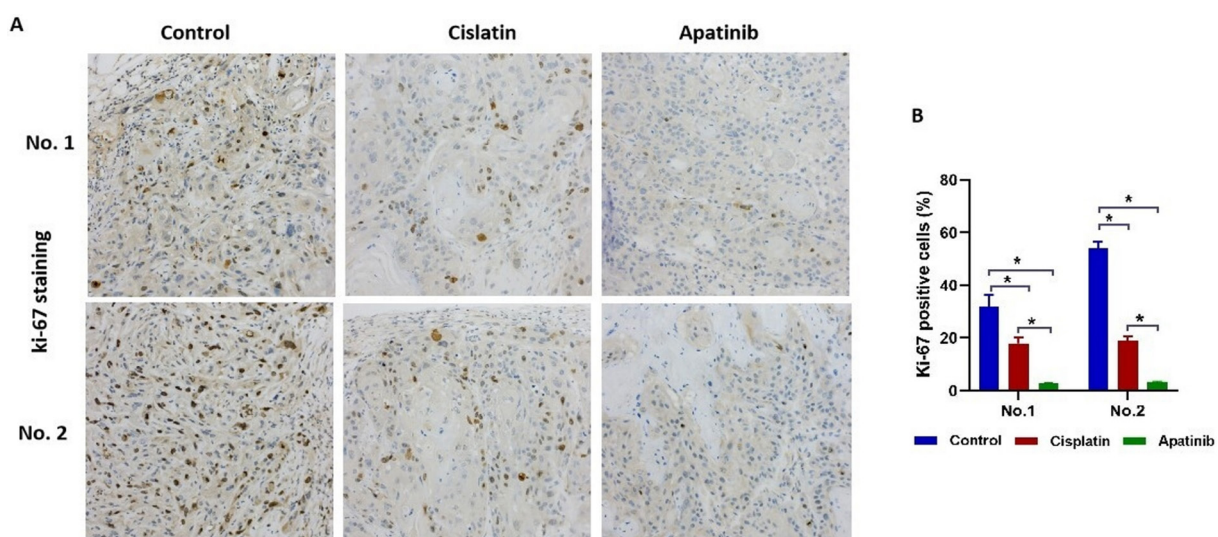


Figure 6: Apatinib Suppresses Tumor Cell Proliferation in Tongue Cancer PDX Models (Assessed by Ki-67 Immunohistochemistry). (A) Images show immunohistochemical (IHC) staining for Ki-67 in PDX model tumor tissues across the control, cisplatin, and apatinib treatment groups for two different patient samples (No. 1 and No. 2). The nuclear protein Ki-67 is stained in clay red or brown ($\times 200$). (B) Bar graph illustrates the Ki-67-positive cell rate in the various groups for both patient samples. The apatinib group shows significantly lower Ki-67-positive cell rates compared to the control and cisplatin groups ($*P<0.05$).

CD31 is a vascular endothelial marker that can be used to evaluate angiogenesis in tumors. In the apatinib group, the MVD was 0.88 ± 0.07 and 0.21 ± 0.06 in experiments No. 1 and No. 2, respectively. These values were significantly lower than those in the cisplatin group (1.54 ± 0.13 in experiments No. 1 and 0.91 ± 0.09 in No. 2) and the control group (4.30 ± 0.34 in experiments No. 1 and 3.31 ± 0.38 in No. 2). These data suggested that apatinib may exert its anti-cancer activity by

Apatinib Inhibits Tumor Cell Proliferation

The Ki-67-positive cell rates in the apatinib group were significantly lower than those in both the cisplatin and control groups across two independent experiments. Specifically, the rates were $2.75 \pm 0.28\%$ (Experiment No. 1) and $3.39 \pm 0.26\%$ (Experiment No. 2) for apatinib, compared to $17.94 \pm 2.18\%$ (Experiment No. 1) and $18.98 \pm 1.57\%$ (Experiment No. 2) for cisplatin, and $32.05 \pm 4.34\%$ and $53.99 \pm 2.62\%$

for the control group, respectively. This difference was statistically significant ($P=0.047$) (figure 6).

Discussion

Our study successfully established two patient-derived xenograft (PDX) models of tongue cancer, which are critical tools for preclinical research. PDX models offer several advantages over traditional cell line models, as they retain the histological characteristics, tumor microenvironment, and genetic heterogeneity of the primary tumor.¹⁵ This makes them highly relevant for evaluating the efficacy of anticancer therapies and predicting clinical outcomes.^{16, 17}

The success rate of PDX model construction is influenced by multiple factors associated with the primary tumor, including tumor invasion, recurrence status, primary or metastatic status, and the degree of immune deficiency in various mouse strains. In our study, fresh tumor tissues from two patients with different histological subtypes of tongue squamous cell carcinoma were used to establish the PDX models. The use of immunodeficient mice ensured a high success rate of tumor engraftment and growth. This approach is similar to that used by Maletzki in 2020 in pancreatic cancer PDX models.¹⁸ Female BALB/c nude mice were selected for this study because they can survive for extended periods under low survival conditions and have a high tumor formation ratio. Additionally, the significant variation in sex hormone levels among female mice may influence tumor growth.¹⁹

Compared to other studies utilizing PDX models, our work specifically targets tongue cancer. For instance, a study by Ju and colleagues in 2022 explored the combination of apatinib with anti-PD-1 therapy in oral squamous cell carcinoma, highlighting the potential of apatinib in head and neck cancers.¹¹ Our study provides a more focused evaluation of apatinib's effects on tongue cancer, which is crucial given the distinct biological behaviors and treatment challenges associated with this cancer type.

The histological consistency between the PDX models and the original patient tumors was confirmed by hematoxylin–eosin (H&E) staining, which showed similar differentiation, keratinization, and nuclear atypia. Furthermore, PCR analysis demonstrated the presence of human-specific genes in the PDX model tumor tissues, confirming their human origin.

Tumor angiogenesis plays a key role in the occurrence of solid tumors.²⁰ The unlimited growth of malignant tumors requires the formation of dense new vascular networks to support the nourishment and growth of tumor tissues, which has also been

proven in our study. Therefore, targeted antitumor angiogenesis therapy has become one of the main research fields in tumor-targeted therapy.²¹ Vascular endothelial growth factor (VEGF) can effectively promote angiogenesis.²² It triggers downstream signaling by activating related VEGF receptor (VEGFR) tyrosine kinases (VEGFR1, VEGFR2, and VEGFR3).

Apatinib inhibits the formation of tyrosine kinases via highly selective competition for the adenosine triphosphate binding sites of VEGFR-2 in cells and blocks the signaling pathway mediated by VEGF binding to its receptor, thereby inhibiting the formation of new blood vessels in tumor tissues to achieve its antitumor function.^{23, 24} In this experiment, the number of CD31-positive blood vessels was reduced in the apatinib group, which indicated that apatinib could inhibit angiogenesis in tongue cancer. Moreover, the weight of the mice did not change significantly; thus, the drug did not produce severe side effects, and it provided a certain degree of protection for the mice.^{25, 26}

Ki-67 is a nuclear antigen encoded by the MKI-67 gene, which is expressed in proliferating cells, and indicates the degree of cell proliferation activity.²⁷⁻²⁹ It is also one of the most reliable indicators for detecting tumor cell proliferation activity.^{30, 31} In this study, Ki-67-positive cells were reduced in the apatinib group, indicating that apatinib exerted an antiproliferative effect. Therefore, we speculated that apatinib may inhibit the growth of tongue cancer by inhibiting angiogenesis and cancer cell proliferation, which in turn inhibits tumor proliferation. Our findings are consistent with previous evidence that apatinib exerts broad antitumor activity in gastric cancer and other malignancies.⁶ Despite the promising results, our study has limitations including: (1) a small sample size ($n=2$ PDX models) limiting generalizability, necessitating expanded cohorts with diverse tongue cancer subtypes to comprehensively evaluate apatinib's efficacy across molecular profiles; (2) mechanistic constraints to basic angiogenesis (CD31) and proliferation (Ki-67) markers, warranting deeper investigation into VEGF/VEGFR-2 signaling, apoptosis regulators, and multi-omics profiling (e.g., RNA-seq) to elucidate apatinib's mode of action and identify resistance markers; (3) the use of subcutaneous PDX models that inadequately replicate the tongue microenvironment, highlighting the need for validation in clinically relevant orthotopic models.

Conclusion

In summary, apatinib exhibited potent antitumor

activity against tongue cancer in PDX models by suppressing angiogenesis and tumor cell proliferation. These results, while promising, were derived from a limited sample of patient-derived tumors and warrant validation in larger PDX cohorts. The work established PDX models as a feasible platform for tongue cancer drug screening but highlighted the necessity of deeper mechanistic exploration in future studies. Apatinib represented a clinically translatable candidate for tongue cancer therapy, pending further investigation of its efficacy across diverse molecular subtypes.

Acknowledgment

This study was supported by Nanchang Royo Biotech Co., Ltd, for the technical assistance, and by the Jiangxi Provincial Natural Science Foundation (Grant No. 20202BABL206067 to XP Hu).

Authors' Contribution

Conception and design: Y.H, X.H; Administrative support: X.H; Provision of study materials or patients: Y.S, Y.X; Collection and assembly of data: Y.S, Y.X; Data analysis and interpretation: Y.S, Y.H, Y.L; All authors contributed to the manuscript writing and commented on previous versions of the manuscript. All authors have read and approved the final manuscript and agree to be accountable for all aspects of the work in ensuring that questions related to the accuracy or integrity of any part of the work are appropriately investigated and resolved.

Declaration of AI

Artificial intelligence tools (specifically DEEPSEEK and KIMI) were used solely for language polishing and grammatical correction during manuscript preparation. No AI systems were involved in data collection, analysis, interpretation, or figure creation. All scientific content and conclusions remain the responsibility of the authors.

Conflict of Interest: None declared.

References

- 1 Sakr Y, Hamdy O, Eldeghedi M, Abdelaziz R, Med Sidi El Moctar E, Alharazin M, et al. Shifting epidemiology trends in tongue cancer: A retrospective cohort study. *Cancers (Basel)*. 2023;15:5680. doi: 10.3390/cancers15235680. PubMed PMID: 38067383; PubMed Central PMCID: PMC10705286.
- 2 Li Y, Chu C, Hu C. Effects of surgery on survival of patients aged 75 years or older with oral tongue squamous cell carcinomas. *Sci Rep.* 2021;11:6003. doi: 10.1038/s41598-021-85647-y. PubMed PMID: 33727684; PubMed Central PMCID: PMC7966770.
- 3 Abdolahi S, Ghazvinian Z, Muhammadnejad S, Saleh M, Asadzadeh Aghdaei H, Baghaei K. Patient-derived xenograft (PDX) models, applications and challenges in cancer research. *J Transl Med.* 2022;20:206. doi: 10.1186/s12967-022-03405-8. PubMed PMID: 35538576; PubMed Central PMCID: PMC9088152.
- 4 Yoshida GJ. Applications of patient-derived tumor xenograft models and tumor organoids. *J Hematol Oncol.* 2020;13:4. doi: 10.1186/s13045-019-0829-z. PubMed PMID: 31910904; PubMed Central PMCID: PMC6947974.
- 5 Xu X, Kumari R, Zhou J, Chen J, Mao B, Wang J, et al. A living biobank of matched pairs of patient-derived xenografts and organoids for cancer pharmacology. *PLoS One.* 2023;18:e0279821. doi: 10.1371/journal.pone.0279821. PubMed PMID: 36602988; PubMed Central PMCID: PMC9815646.
- 6 Fathi Maroufi N, Rashidi MR, Vahedian V, Akbarzadeh M, Fattahi A, Nouri M. Therapeutic potentials of apatinib in cancer treatment: Possible mechanisms and clinical relevance. *Life Sci.* 2020;241:117106. doi: 10.1016/j.lfs.2019.117106. PubMed PMID: 31786193.
- 7 Wang L, Li W, Liu YG, Zhang C, Gao WN, Gao LF. Clinical efficacy and safety of bevacizumab, apatinib, and recombinant human endothelial inhibitor in the treatment of advanced gastric cancer. *J Oncol.* 2022;2022:6189833. doi: 10.1155/2022/6189833. PubMed PMID: 35251174; PubMed Central PMCID: PMC8894022.
- 8 Li H, Huang H, Zhang T, Feng H, Wang S, Zhang Y, et al. Apatinib: A novel antiangiogenic drug in monotherapy or combination immunotherapy for digestive system malignancies. *Front Immunol.* 2022;13:937307. doi: 10.3389/fimmu.2022.937307. PubMed PMID: 35844616; PubMed Central PMCID: PMC9276937.
- 9 Zhao L, Peng Y, He S, Li R, Wang Z, Huang J, et al. Apatinib induced ferroptosis by lipid peroxidation in gastric cancer. *Gastric Cancer.* 2021;24:642-54. doi: 10.1007/s10120-021-01159-8. PubMed PMID: 33544270.
- 10 Li Z, Zhou X, Wang S, Shi L, Meng R, Dai X, et al. The efficacy and safety of apatinib

in patients with heavily pretreated end-stage cancer: a retrospective study. *Transl Cancer Res.* 2023;12:904-12. doi: 10.21037/tcr-22-2080. PubMed PMID: 37180651; PubMed Central PMCID: PMC10174995.

11 Ju W-t, Xia R-h, Zhu D-w, Dou S-j, Zhu G-p, Dong M-j, et al. A pilot study of neoadjuvant combination of anti-PD-1 camrelizumab and VEGFR2 inhibitor apatinib for locally advanced resectable oral squamous cell carcinoma. *Nat Commun.* 2022;13:5378. doi: 10.1038/s41467-022-33080-8.

12 Xin Y, Li S, Jiang Q, Hu F, He Y, Zhang J. Establishment of a jaw fibrosarcoma patient-derived xenograft and evaluation of the tumor suppression efficacy of plumbagin against jaw fibrosarcoma. *Front Oncol.* 2020;10:1479. doi: 10.3389/fonc.2020.01479. PubMed PMID: 32974176; PubMed Central PMCID: PMC7481444.

13 Hu F, Guo L, Yu J, Dai D, Xiong Y, He Y, et al. Using patient-derived xenografts to explore the efficacy of treating head-and-neck squamous cell carcinoma with anlotinib. *Pathol Oncol Res.* 2021;27:1610008. doi: 10.3389/pore.2021.1610008. PubMed PMID: 34955687; PubMed Central PMCID: PMC8696349.

14 Kvietkauskas M, Zitkute V, Leber B, Strupas K, Stiegler P, Schemmer P. Dietary melatonin and glycine decrease tumor growth through antiangiogenic activity in experimental colorectal liver metastasis. *Nutrients.* 2021;13:2035. doi: 10.3390/nu13062035. PubMed PMID: 34199311; PubMed Central PMCID: PMC8231877.

15 Chen L, Pan X, Zhang YH, Hu X, Feng K, Huang T, et al. Primary tumor site specificity is preserved in patient-derived tumor xenograft models. *Front Genet.* 2019;10:738. doi: 10.3389/fgene.2019.00738. PubMed PMID: 31456818; PubMed Central PMCID: PMC6701289.

16 Guo S, Gao S, Liu R, Shen J, Shi X, Bai S, et al. Oncological and genetic factors impacting PDX model construction with NSG mice in pancreatic cancer. *FASEB J.* 2019;33:873-84. doi: 10.1096/fj.201800617R. PubMed PMID: 30091943.

17 Xu W, Zhao ZY, An QM, Dong B, Lv A, Li CP, et al. Comprehensive comparison of patient-derived xenograft models in hepatocellular carcinoma and metastatic liver cancer. *Int J Med Sci.* 2020;17:3073-81. doi: 10.7150/ijms.46686. PubMed PMID: 33173428; PubMed Central PMCID: PMC7646096.

18 Maletzki C, Bock S, Fruh P, Macius K, Witt A, Prall F, et al. NSG mice as hosts for oncological precision medicine. *Lab Invest.* 2020;100:27-37. doi: 10.1038/s41374-019-0298-6. PubMed PMID: 31409886.

19 Fan X, Wu L, Cheng T, Lv W, Tian J, Tao J, et al. Oroxylin A may promote cell apoptosis and inhibit epithelial-mesenchymal transition in endometrial cancer, associated with the ER β /PI3K/AKT pathway. *Sci Rep.* 2025;15:12225. doi: 10.1038/s41598-025-97122-z. PubMed PMID: 40211010; PubMed Central PMCID: PMC11986019.

20 Al-Ostoot FH, Salah S, Khamees HA, Khanum SA. Tumor angiogenesis: Current challenges and therapeutic opportunities. *Cancer Treat Res Commun.* 2021;28:100422. doi: 10.1016/j.ctarc.2021.100422. PubMed PMID: 34147821.

21 Xie YH, Chen YX, Fang JY. Comprehensive review of targeted therapy for colorectal cancer. *Signal Transduct Target Ther.* 2020;5:22. doi: 10.1038/s41392-020-0116-z. PubMed PMID: 32296018; PubMed Central PMCID: PMC7082344.

22 Liu Y, Long L, Zhang F, Hu X, Zhang J, Hu C, et al. Microneedle-mediated vascular endothelial growth factor delivery promotes angiogenesis and functional recovery after stroke. *J Control Release.* 2021;338:610-22. doi: 10.1016/j.jconrel.2021.08.057. PubMed PMID: 34481025.

23 Kang R, Song M, Fang Z, Liu K. Nano-composite hydrogels of Cu-Apa micelles for anti-vasculogenic mimicry. *J Drug Target.* 2023;31:166-78. doi: 10.1080/1061186x.2022.2115047. PubMed PMID: 35993258.

24 Tao K, Chen C, Xu G, Tao F, He M. Low-dose apatinib optimizes the vascular normalization and enhances the antitumor effect of PD-1 inhibitor in gastric cancer. *Transl Cancer Res.* 2024;13:4290-300. doi: 10.21037/tcr-23-2328. PubMed PMID: 39262493; PubMed Central PMCID: PMC11385532.

25 Liu X, Xu J, Li F, Liao Z, Ren Z, Zhu L, et al. Efficacy and safety of the VEGFR2 inhibitor apatinib for metastatic soft tissue sarcoma: Chinese cohort data from NCT03121846. *Biomed Pharmacother.* 2020;122:109587. doi: 10.1016/j.bioph.2019.109587. PubMed PMID: 31786466.

26 Tenyi A, Milutinović A, Nemeth L. Expression of CD31, CD34, and smooth muscle actin (SMA) in endothelial cells of dental pulp vessels. *Biomol Biomed.* 2023;24:821-6. doi: 10.17305/bb.2023.9988. PubMed PMID: 38153414; PubMed Central PMCID: PMC11293224.

27 Gerdes J, Schwab U, Lemke H, Stein H.

Production of a mouse monoclonal antibody reactive with a human nuclear antigen associated with cell proliferation. *Int J Cancer.* 1983;31:13-20. doi: 10.1002/ijc.2910310104. PubMed PMID: 6339421.

28 Schwiebs A, Faqar-Uz-Zaman F, Herrero San Juan M, Radeke HH. S1P lyase regulates intestinal stem cell quiescence via Ki-67 and FOXO3. *Int J Mol Sci.* 2021;22:5682. doi: 10.3390/ijms22115682. PubMed PMID: 34073605; PubMed Central PMCID: PMC8198365.

29 Lei HJ, Wang SY, Chau IY, Li AF, Chau YP, Hsia CY, et al. Hepatoma upregulated protein and Ki-67 expression in resectable hepatocellular carcinoma. *J Chin Med Assoc.* 2021;84:623-32. doi: 10.1097/jcma.0000000000000540. PubMed PMID: 33883465.

30 Li Z, Li F, Pan C, He Z, Pan X, Zhu Q, et al. Tumor cell proliferation (Ki-67) expression and its prognostic significance in histological subtypes of lung adenocarcinoma. *Lung Cancer.* 2021;154:69-75. doi: 10.1016/j.lungcan.2021.02.009. PubMed PMID: 33626488.

31 Atrash S, Robinson M, Taneja A, Paul B, Cassetta K, Ndiaye A, et al. Bone marrow Ki-67 index is of prognostic value in newly diagnosed multiple myeloma. *Eur J Haematol.* 2023;111:373-81. doi: 10.1111/ejh.14016. PubMed PMID: 37311695.